Untargeted LC-HRMS applied to microcystin-producing cyanobacterial cultures for the evaluation of the efficiency of chlorine-based treatments commonly used for water potabilization

Mara Simonazzi [a,c,*], Antonella Miglione [b], Luciana Tartaglione [b,**], Michela Varra [b], Carmela DellAversano [b,c], Franca Guerrini [a], Rossella Pistocchi [a], Laura Pezzolesi [a,c]

[a] Department of Biological, Geological and Environmental Sciences (BiGeA), University of Bologna, Via Sant'Alberto 163, 48123, Ravenna, Italy
[b] Department of Pharmacy, School of Medicine and Surgery, University of Naples Federico II, Via D. Montesano 49, 80131, Naples, Italy
[c] NBFC, National Biodiversity Future Center, Palermo, 90133, Italy

HIGHLIGHTS

- Sodium hypochlorite inactivated *M. aeruginosa* at lower doses than chlorine dioxide.
- The two oxidants acted differently on intracellular toxins and metabolites release.
- Untargeted LC-HRMS allowed the discovery of two new cyanopeptolin-type peptides.

GRAPHICAL ABSTRACT
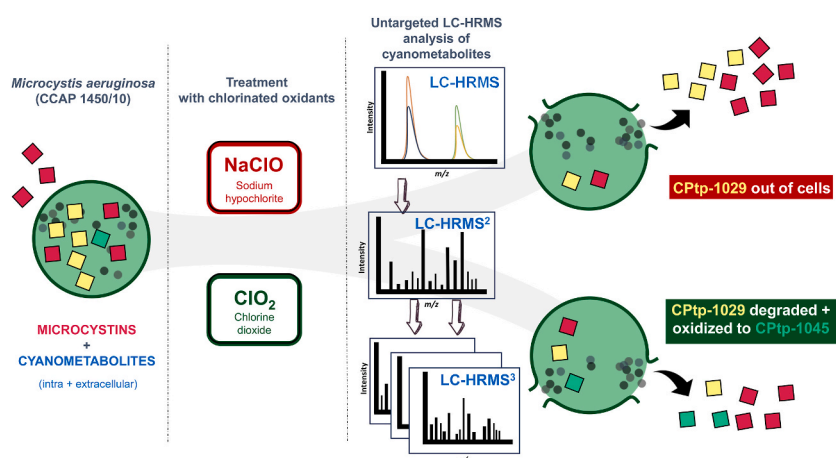
ARTICLE INFO

ABSTRACT

Cyanobacteria in water supplies are considered an emerging threat, as some species produce toxic metabolites, cyanotoxins, of which the most widespread and well-studied are microcystins. Consumption of contaminated water is a common exposure route to cyanotoxins, making the study of cyanobacteria in drinking waters a priority to protect public health. In drinking water treatment plants, pre-oxidation with chlorinated compounds is widely employed to inhibit cyanobacterial growth, although concerns on its efficacy in reducing cyanotoxin content exists. Additionally, the effects of chlorination on abundant but less-studied cyanometabolites (e.g. cyanopeptolins whose toxicity is still unclear) remain poorly investigated. Here, two chlorinated oxidants, sodium hypochlorite (NaClO) and chlorine dioxide (ClO$_2$), were tested on the toxic cyanobacterium *Microcystis*

---

* Corresponding author.
** Corresponding author.
 E-mail addresses: mara.simonazzi2@unibo.it (M. Simonazzi), luciana.tartaglione@unina.it (L. Tartaglione).

aeruginosa, evaluating their effect on cell viability, toxin profile and content. Intra- and extracellular microcystins and other cyanometabolites, including their degradation products, were identified using an untargeted LC-HRMS approach. Both oxidants were able to inactivate *M. aeruginosa* cells at a low dose (0.5 mg L^{-1}), and greatly reduced intracellular toxins content (>90%), regardless of the treatment time (1–3 h). Conversely, a two-fold increase of extracellular toxins after NaClO treatment emerged, suggesting a cellular damage. A novel metabolite named cyanopeptolin-type peptide-1029, was identified based on LC-HRMS^n (n = 2, 3) evidence, and it was differently affected by the two oxidants. NaClO led to increase its extracellular concentration from 2 to 80–100 μg L^{-1}, and ClO$_2$ induced the formation of its oxidized derivative, cyanopeptolin-type peptide-1045. In conclusion, pre-oxidation treatments of raw water contaminated by toxic cyanobacteria may lead to increased cyanotoxin concentrations in drinking water and, depending on the chemical agent, its dose and treatment duration, also of oxidized metabolites. Since the effects of such metabolites on human health remain unknown, this issue should be handled with extreme caution by water security agencies involved in drinking water management.

1. Introduction

Cyanobacteria represent major constituents of phytoplankton in aquatic ecosystems, contributing to 20–30% of the global primary production (de la Cruz et al., 2020). Under certain environmental conditions (e.g., high nutrient levels, water temperature, and light intensity), cyanobacteria can massively proliferate giving rise to harmful cyanobacterial blooms. Several studies highlight a close correlation between climate changes and the increasing magnitude, frequency and duration of cyanobacterial blooms (Huisman et al., 2018). Additionally, many cyanobacteria genera such as *Microcystis* and *Planktothrix* produce toxic metabolites (i.e., cyanotoxins) characterized by different chemical structures and mechanisms of action (Buratti et al., 2017). Microcystins (MCs) are one of the most studied cyanotoxins (Wang et al., 2022), which exert hepatotoxic effects by targeting liver cells and inducing the inhibition of protein phosphatases, and may also act as tumor promoters (Fastner and Humpage, 2021). Among the more than 300 known MCs variants (Jones et al., 2021), MC-LR - containing leucine and arginine in positions 2 and 4 - is considered the most common and toxic one (LD$_{50}$ i. p. injection = 50 and 160–300 μg kg^{-1} for MC-LR and other MCs variants, respectively Fastner and Humpage, 2021). Nonetheless, different and less-studied bioactive metabolites are produced by cyanobacteria, such as other peptides, e.g., cyanopeptolins and cyanopeptolin-type peptides (CPtps), which comprise more than 230 cyclic hexapeptides containing a β-lactone ring and featuring a characteristic 3-amino-6-hydroxy-2-piperidone (Ahp) moiety (Konkel et al., 2023; McDonald et al., 2021). Despite cyanopeptides may occur in freshwater at concentrations similar to those reported for the well-studied MCs (Beversdorf et al., 2017), they have been poorly investigated from both a chemical and a toxicological stand point. Cyanopeptides should not be neglected during water surveillance as a potential ecotoxicity has recently emerged, due to a general inhibition effect on enzymes (proteases, trypsin, chymotrypsin, aminopeptidase among others) in micro-to nanomolar range and toxic effects in the same range of MCs when tested in biological assays (Janssen, 2019). In routine analyses, liquid chromatography coupled to mass spectrometry (LC-MS) is employed in targeted screening of selected cyanotoxins, whose reference standards are available, while no information can be easily obtained for other unknown cyanometabolites. More recently, approaches based on the untargeted analysis using LC-high-resolution mass spectrometry (LC-HRMS), together with an ever-growing comprehensive database of cyanobacterial metabolites (Janssen et al., 2023), have been successfully used for toxic profile determination of bloom material and cultured strains (Kust et al., 2020; Varriale et al., 2023).

In the perspective of the global safe management of drinking water supplies, cyanobacteria monitoring in water bodies for human consumption is a priority (Moreira et al., 2022), and national regulations are in place to prevent the risks associated with cyanotoxins' exposure. For instance, in Europe, the EU 2020/2184 directive includes MC-LR among the contaminants to be monitored (the maximum allowed concentration of total MCs in drinking water is set at 1.0 μg L^{-1}).

Cyanobacteria may negatively affect the efficiency of drinking water treatment plants (DWTPs), in which several methods are employed, typically including coagulation, flocculation, sedimentation, filtration, and final disinfection (Jalili et al., 2022). Cyanobacteria biomass can cause filtration-clogging action or the increasing coagulant and flocculants demand, as well as the overloading of other downstream processes such as absorption on activated carbons (Jalili et al., 2022; Zamyadi et al., 2013), or lead to the presence of cells and toxins within DWTPs or in finished water if cyanobacteria breakthrough occurs (Mohamed, 2016; Pazouki et al., 2016; Rose et al., 2018). Even overcoming the difficulties arising from the presence of cyanobacterial biomass, the dispersed cyanobacteria cells can negatively affect DWTPs. Evidence of cyanobacterial cells' accumulation, survival and even growth in the settling sludges arising in the water treatment chain have been reported. This phenomenon can cause cell damages, thus determining the increase of dissolved toxins' concentration in the water under treatment (Jalili et al., 2022; Pestana et al., 2016). Another common step in water treatment is the pre-oxidation of raw water using oxidant disinfectants, specifically added to inactivate or kill waterborne pathogens (Betancourt and Rose, 2004). Because of their relatively low costs, ready-availability, and wide-spectrum applications, chlorinated oxidants (chlorine dioxide, sodium hypochlorite, chloramines) are the most used disinfectants in DWTPs. However, pre-oxidation of raw water poses concerns about the chlorinated oxidants-driven formation of disinfection by-products (DBPs) such as carcinogenic trihalomethanes (Mazhar et al., 2020). Furthermore, when toxic cyanobacteria are present, pre-oxidation may cause cell lysis and consequently extracellular toxin release (Li et al., 2020; Zamyadi et al., 2013; Zhang et al., 2017). Despite that, data suggested that pre-oxidation prior to flocculation and sedimentation may favor the removal of algal and cyanobacterial cells (Qi et al., 2021). Accordingly, the use of low doses of oxidants during pre-oxidation (<2.0 mg L^{-1}) of raw water has been suggested to achieve the inactivation of cells without causing lyses resulting in toxin release (Henderson et al., 2008; Jalili et al., 2022). In this complex scenario, is noteworthy that a pre-oxidation step may be required by national laws (i.e., in Italy; Italian Legislative Decree 152/2006, 2006) and consequently, a careful evaluation of the related benefits and risks should be done. The present study aims to investigate the effects of low-dosed chlorinated oxidants commonly employed in DWTPs, i.e., sodium hypochlorite and chlorine dioxide, on cultures of the toxic cyanobacterium *Microcystis aeruginosa*. The effects of the oxidants in inhibiting cyanobacterial cell viability and on intra-cellular toxin content and their extra-cellular release were assessed. In this frame, metabolites produced by *M. aeruginosa* were explored by analyzing cultures before and after the treatments by an untargeted LC-HRMS approach.

2. Materials and methods

2.1. Chemicals

All reagents, solvents, and chemical standards used were of

analytical grade or higher. HPLC grade solvents (water, acetonitrile, methanol) and formic acid (reagent grade, ≥99.5%) used for LC-HRMS analyses were from Merck KGaA (Darmstadt, Germany). Chlorine dioxide stock solution of 146 mg L^{-1} (ClO$_2$) was prepared ready-to-use by the water treatment Company (Romagna Acque – Società delle Fonti S.p. A.), within a dedicated reactor by combining hydrochloric acid (33%) and sodium chlorite (25%), and the concentration was determined spectrophotometrically at λ = 445 nm. A commercial solution of sodium hypochlorite 15% (NaClO) was purchased ready-made (Società Chimica Bussi S.p.A.). Both oxidants were accordingly dosed for preliminary tests and for oxidation experiments to obtain a final concentration in the range 0.1–2.0 mg L^{-1}. Sodium thiosulfate 1% (w/v) was prepared by dissolving 1 g of sodium thiosulphate in 100 mL of distilled water. Certified Reference Material (CRM) of MC-LR (10.3 μg mL^{-1}), [Dha^7] MC-LR (9.4 μg mL^{-1}), and MC-RR (10.1 μg mL^{-1}) were purchased from the National Research Council of Canada (Halifax, Canada).

2.2. Cyanobacterial strain and culture conditions

M. aeruginosa (CCAP 1450/10) was obtained from the Culture Collection of Algae and Protists (Scottish Marine Institute, Oban, UK) and grown in 0.2 L glass flasks in BG11 medium (Stanier et al., 1971), at a temperature of 20 ± 1 °C, light intensity 90–120 μmol m^{-2} s^{-1}, with a photoperiod of 16:8 h light:dark. Cultures were scaled-up at the same growing conditions for subsequent experiments using chlorinated oxidants. Prior to oxidation experiments, pH was adjusted to 7.0 ± 0.5 with hydrochloric acid (1.0 M).

2.3. Application of chlorinated oxidants on M. aeruginosa cultures for EC$_{50}$ evaluation

Cultures of *M. aeruginosa* at exponential growth phase were diluted with demineralized water to reach a cell density of 300 × 10^6 cell L^{-1}. The cell concentration of the cyanobacterial suspension was chosen to clearly evaluate the maximum observed effect caused by chlorinated oxidants on photosynthetic efficiency, a parameter widely used to assess algae and cyanobacteria viability in toxicological studies involving photosynthetic organisms. The two chlorinated oxidants, ClO$_2$ and NaClO, were preliminarily applied at increasing concentrations in the range of 0.0–4.0 mg L^{-1} (treatment time 1 h), then, a narrower range of concentrations for each oxidant (0.0–2.0 mg L^{-1} and 0.0–1.0 mg L^{-1} for ClO$_2$ and NaClO, respectively), was chosen to treat cultures (n = 3). After 1 h and 24 h of each treatment, aliquots of each sample (3 mL) were dark-adapted for 15–20 min and subsequently analyzed by a pulse amplitude-modulated fluorometer, model 101-PAM (H. Walz, Effeltrich, Germany). The photosynthetic efficiency was measured in terms of maximum and effective quantum yield of photosystem II (ΦPSII and Φ'PSII, respectively), and the half maximal effective concentration (EC$_{50}$) of the two chlorinated oxidants upon both ΦPSII and Φ'PSII was determined by fitting dose-response curves into a log-logistic model, using fluorometer's settings and calculations previously described (Pichierri et al., 2016), as follows:

$$y = \frac{top - bot}{1 + (Ox/EC_{50})^c}$$

Where:

    y = endpoint value.

    Ox = oxidant concentration

    bot = expected endpoint value when the concentration of the oxidant is infinite (bottom asymptote)

    top = expected endpoint value when the concentration of the oxidant is zero (topasymptote)

    c = slope.

2.4. Oxidation experiment

M. aeruginosa cultures were scaled up to 10 L and collected at the exponential growth phase. The high cell density culture was gently mixed and divided into 0.5 L glass flasks for a total of 21 replicates (n = 3, for both control and each treatment). Before the oxidation experiment, each flask was diluted with demineralized water to reach a final cell density of 120 × 10^6 cell L^{-1}. This cell density was lower than the one tested for the EC$_{50}$ experiment, and it was chosen to simulate a cyanobacterial density closer to natural conditions. Solutions of the chlorinated oxidants NaClO or ClO$_2$ were directly added to each flask to obtain a final dose of 0.5 mg L^{-1}, which was chosen based on the previously calculated EC$_{50}$ (section 2.3). For ClO$_2$, a higher dose of 2.0 mg L^{-1} was also tested. Each combination of oxidant and dose was tested with a treatment time of 1 and 3 h versus controls. The oxidation experiments were conducted at room temperature in semi-dark conditions, to avoid direct exposure to light, and the flasks were gently mixed every 30 min. At the end of each exposure time, sodium thiosulfate solution (1% w/v) was added to quench the chemical oxidation.

2.5. Effect of the oxidants on cyanobacterial cells

The potential of each oxidant to inactivate the cyanobacterial cells was estimated by measuring photosynthetic efficiency and cell density. Sample aliquots (5 mL) were taken from each replicate to determine the maximum quantum yield of PSII as previously described (section 2.3). Remaining samples were preserved with Lugol's iodine solution for subsequent cell enumeration (Utermöhl, 1931) using an inverted light microscope at 320x magnification (ZEISS Axiovert 100). The total number of cells following the oxidation treatments was compared to those of the untreated controls and expressed as percentage (%)(von Sperling et al., 2020).

2.6. Toxins extraction

Immediately after the addition of sodium thiosulfate, each replicate (controls and treatments with NaClO (0.5 mg L^{-1}) 1h, NaClO (0.5 mg L^{-1}) 3h, ClO$_2$ (0.5 mg L^{-1}) 1h, ClO$_2$ (0.5 mg L^{-1}) 3h, ClO$_2$ (2.0 mg L^{-1}) 1h, ClO$_2$ (2.0 mg L^{-1}) 3h) was centrifuged (6500×g, 10 min) to separate water from cyanobacterial biomass, from now on referred to as extracellular and intracellular fraction, respectively. Each extracellular fraction (500 mL) was extracted by solid phase extraction (SPE) using Oasis HLB cartridges (6 mL capacity, Waters, Milford, MA, USA) and eluting the samples with 4 mL of methanol, according to the procedure described in Kaloudis et al. (2013). The obtained eluates were evaporated under a gentle nitrogen stream until dryness. Each intracellular fraction was extracted according to an optimized protocol for fresh material (Christophoridis et al., 2018). Briefly, 1.5 mL of 75% aqueous methanol (v/v) was added to each test tube containing cyanobacterial biomass, vortexed, and sonicated in an ultrasonic bath for 15 min. The sonicated samples were then centrifuged (2550×g, 10 min at room temperature) and the supernatants collected. The procedure was repeated a second time using the same solvent mixture and volume, and a third time using 1.5 mL of n-butanol. The resulting three supernatants were combined and dried under a gentle nitrogen stream. Dried samples were kept at −20 °C until LC-HRMS analyses. Each extracellular and intracellular dried fraction was reconstituted with 500 μL of 20% aqueous methanol and analyzed by LC-HRMS.

2.7. Untargeted LC-HRMS analyses of cyanotoxins and other cyanobacterial metabolites

LC–HRMS analyses were carried out using an Ultimate 3000 quaternary system coupled to a hybrid linear ion trap LTQ–Orbitrap XL™ Fourier transform MS equipped with an ESI ION MAX source (SN 01719B, Thermo-Fisher, San José, USA) using LC-HRMS (*method 1*)

conditions reported in Varriale et al. (2023). Extracted ion chromatograms (XICs) were obtained from HR full-scan MS spectra by selecting the exact masses of $[M+H]^+$ and/or $[M+2H]^{2+}$ ions of all known MCs (± 5 ppm) reported in CyanoMetDB (Jones et al., 2021, the updated versions of the database are available on the Zenodo and NORMAN Suspect List Exchange (No S75)). For the suspected MC variants, precursor ions were selected for targeted $HRMS^2$ experiments in collision induced dissociation (CID) and higher energy collisional dissociation (HCD) modes (isolation width 2.0 m/z, activation Q 0.250, and activation time 30 ms) using a normalized collision energy of 40% (HCD) or 30% (CID). Identification of unknown cyanometabolites was carried out by DDA experiments, by setting up 9 scan events, with scan event 1 being a HR full-scan MS (range m/z 400–1200), and the other 8 scan events being $HRMS^2$ (CID or HCD) of the 8 most intense ions observed in the full-scan MS spectrum. Threshold value of MS^2 acquisition was set as 500 (intensity units). Elemental formulae were calculated based on the mass of the mono-isotopic peak of each ion cluster using Xcalibur v2.2 SP1.48 (Thermo-Fisher) with a mass tolerance of 3–5 ppm.

2.7.1. Quantitation of MCs and cyanopeptolin-type peptides

Each reconstituted intracellular fraction (1:10 dilution in 20% aqueous methanol) and extracellular fraction (1:100 dilution in 20% aqueous methanol) was analyzed by LC–HRMS. Cyanotoxins detected in the samples were MCs containing a single Arg residue and, based on evidence reported by Varriale et al. (2023), quantitation was performed using MC-LR CRM as a reference and assuming similar molar response for all the other variants. Matrix interference on ionization of MC-LR CRM was negligible (Varriale et al., 2023) so, a matrix-free external standard calibration curve of MC-LR (15.6, 31.3, 62.5, 125, 250, 500, 1250 ng mL^{-1}) in methanol–water (1:4, v/v) was prepared from MC-LR CRM stock solution and analyzed by LC–HRMS. Quantitation was accomplished by comparing manually integrated XIC areas of each MC (Table S1) to the MC-LR CRM injected under the same experimental conditions. The instrumental limit of quantitation (LOQ) measured for MC-LR was 5 ng mL^{-1} and, based on extraction efficiency data reported by Christophoridis et al. (2018); Kaloudis et al. (2013) (extraction recoveries from biomass and water in the ranges 91–154% and 70–120%, respectively), the method LOQ for MCs in biomass and water were 0.042 fg $cell^{-1}$ and 0.01 μg L^{-1}, respectively. Quantitative estimation of the two new cyanopeptolin-type peptides, CPtp-1029 at m/z 1030.5246 and CPtp-1045 at m/z 1046.5222, was accomplished following the same approach. Finally, total toxin content was calculated as the sum of each intracellular and relevant extracellular fraction.

2.7.2. Effect of the oxidants on toxin content

The toxin content after each treatment was compared to the toxin content of the control and the observed changes between the two conditions (treatments vs controls) were evaluated as percent toxin variation, i.e., ΔTox(%).

The ΔTox(%) was calculated as follows:

$$\Delta Tox(\%) = \left(\frac{C_{highest} - C_{lowest}}{C_{highest}} \right) \times 100$$

Where C_{lowest} and $C_{highest}$ were the lowest and the highest toxin concentration measured between control and treated samples for each replicate, respectively. The ratio between the lowest and the highest concentration was chosen to obtain positive and comparable values in those case where the content of toxins in the treatments exceeded that of the controls.

2.8. Data analysis

Data analysis was performed on PAST version 4.11 (Hammer et al., 2001) for the comparison of the main evaluated parameters (i.e., cell or toxin concentrations) among the different treatments. EC_{50}

dose-response curves were generated on R version 4.2.0 (R Core Team, 2022). Data homogeneity was evaluated with Levene's test for homoskedasticity and was transformed accordingly prior to further investigation. The effect of the different treatments on the photosynthetic activity, the number of cells, the toxin content and the percent variation were examined by analysis of variance (ANOVA) and Tukey's test for post-hoc comparisons was used when differences were significant ($p < 0.05$).

3. Results

3.1. Photosynthetic efficiency of M. aeruginosa cells treated with oxidants

A preliminary assessment of the effect of the chlorinated oxidants NaClO and ClO_2 on the photosynthetic efficiency of *M. aeruginosa* is reported in Fig. 1. Increasing doses of each oxidant led to a gradual inhibition of the maximum and effective quantum yields of PSII, resulting in values below 20% at the highest tested doses. For both oxidants, a significant reduction than control (ANOVA, $p < 0.05$) was obtained for all concentrations above 0.4 mg L^{-1}, regardless of the treatment time (1 h or 24 h).

The EC_{50} values (i.e., oxidant concentration needed to achieve a 50% inhibition of the two photosynthetic parameters here studied, the maximum and the effective quantum yields of PSII, respectively) obtained were almost two-fold higher for ClO_2-treated samples than for NaClO-treated ones, i.e. 0.50–0.59 vs 0.28–0.34 mg L^{-1}, respectively (Table S2, Fig. S1), indicating how the two oxidants affect differently the cyanobacterial cells. EC_{50} values slightly increased after 24 h compared to 1 h, likely as a result of the higher photosynthetic activity observed after 24 h of treatment with both oxidants (Fig. 1). This evidence suggests that the damages upon the photosynthetic apparatus of *M. aeruginosa* caused by the chlorinated oxidants were reversible at the tested doses.

3.2. Inhibition of photosynthetic efficiency and effects on M. aeruginosa cells following the oxidation experiment

Based on preliminary investigations (section 3.1), *M. aeruginosa* cultures were treated with each oxidant at specific doses and times (i.e., 0.5 mg L^{-1} for 1 and 3 h, and 2.0 mg L^{-1} only for ClO_2), and the effects on the cell viability were evaluated in terms of cell density and photosynthetic activity, obtained from the maximum quantum yield of PSII (Fig. 2). During the oxidation experiment, the number of cells (Fig. 2a) remained unchanged after the NaClO treatment i.e., 121×10^6 vs 129-131×10^6 cell L^{-1} for control and NaClO treatment, respectively (ANOVA, $p > 0.05$), as also indicated by the negative percentages of cells compared to controls (– 6–8%), and by the calculated ratio among the cell density in treated cultures and in controls that was near to 1 (Table S3). This corresponded to a non-significant increase of the cells in NaClO-treated samples, likely due to sampling and to culture natural variability. The cell density significantly decreased only for ClO_2 treatments (32–46%, ANOVA, $p < 0.05$, Table S3), with a major effect at the highest tested dose (2.0 mg L^{-1}) without differences among treatment times (cell density in the range 65-81 $\times 10^6$ cell L^{-1}, Fig. 2a). The photosynthetic efficiency of the cyanobacterium both in terms of maximum (Fig. 2b) and effective quantum yield (Table S3) was inhibited by both oxidants compared to controls, resulting in a residual activity below 20% (ANOVA, $p < 0.05$). Treated cells were checked through environmental scanning electron microscopy (ESEM) imaging, observing a general roughness of cell membranes or their damage compared to controls, especially with NaClO treatment (Fig. S2).

3.3. Relative abundances of toxins in control and treated samples by LC-HRMS

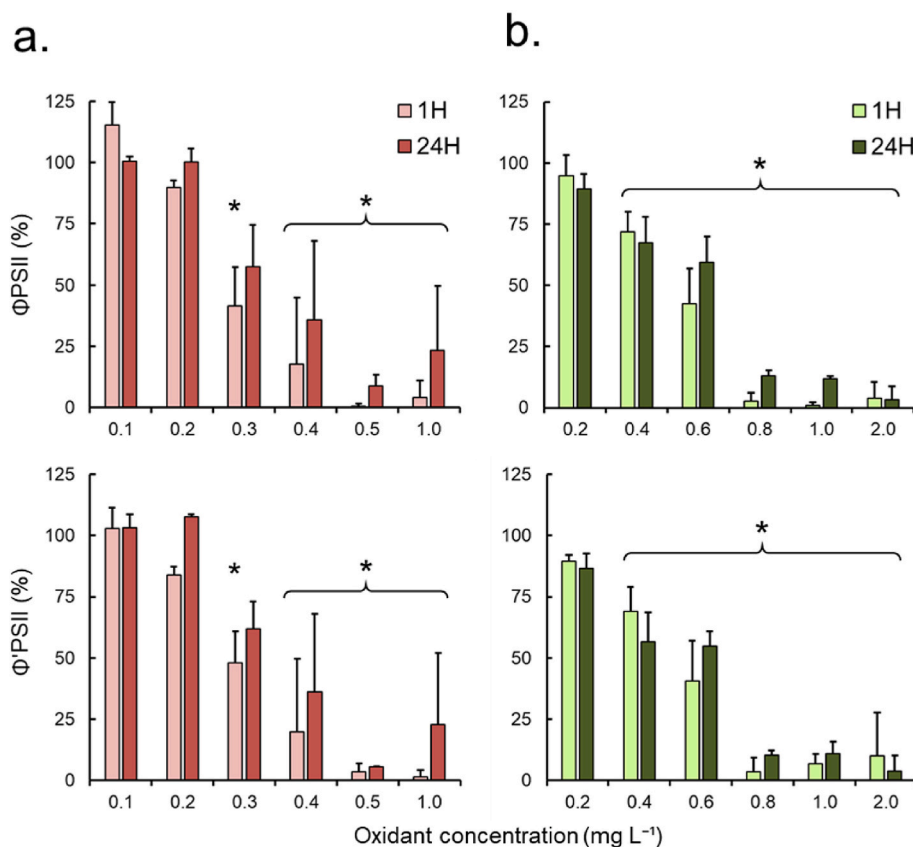The intracellular and extracellular fractions resulting from the

Fig. 1. Photosynthetic activity (%) of *M. aeruginosa* cells treated with increasing doses of the chlorinated oxidants NaClO (a, red) and ClO$_2$ (b, green), after 1 h and 24 h of treatment time. Values are expressed as percent inhibition of the maximum quantum yield (ΦPSII (%), upper graphs) and of the effective quantum yield (Φ'PSII (%), bottom graphs) with respect to the control. Significant differences compared to control are indicated with asterisks (ANOVA, $p < 0.05$). (For interpretation of the references to colour in this figure legend, the reader is referred to the Web version of this article.)
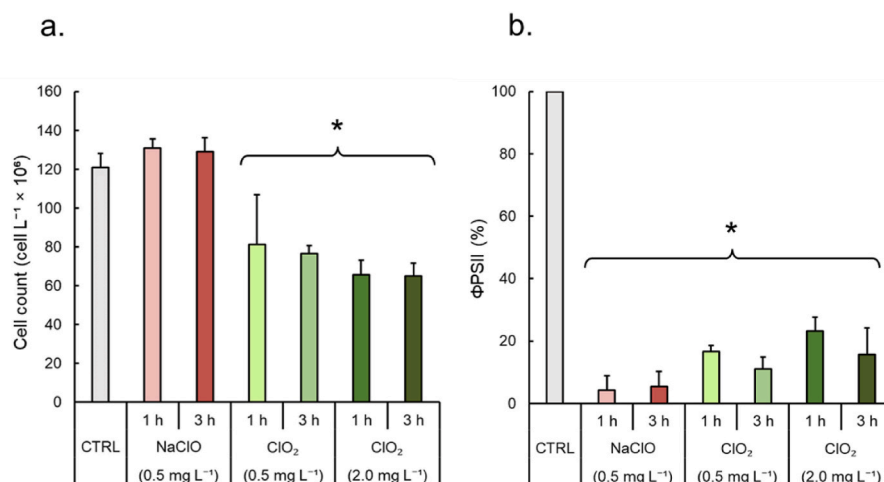

Fig. 2. Effect of NaClO and ClO$_2$ tested at 0.5 and 2.0 mg L^{-1} on cells of *M. aeruginosa* during the oxidation experiment, a) number of cells (cell × 10^6 L^{-1}), and b) photosynthetic activity calculated from maximum quantum yields (ΦPSII (%)). Significant differences compared to control are indicated with asterisks (ANOVA, $p < 0.05$).

centrifugation of each culture (controls and treated ones) were analyzed by LC-HRMS to first evaluate the toxin profile of the tested strain (Fig. 3). An array of microcystins, all featuring a single Arg at position-2, were detected in both *M. aeruginosa* controls and treated cultures (Table S1). The number of Arg residues is a key structural feature influencing the ionization behavior of MCs, particularly MCs containing 1-Arg (e.g., MC-LR) form predominantly [M+H]$^+$ ions and so

quantitation can be accomplished using MC-LR standard assuming a similar molar responses for all the variants. MC-LR and its analogue containing a dehydroalanine in position 7, [Dha^7]-MC-LR, were found to be the two dominant variants representing 18.0% and 5.7% of the intracellular toxin fraction, respectively, followed by MC-LY (1.3%), MC-LF (1.2%), [D-Asp^3]MC-LY (0.4%) and [D-Asp^3]MC-LF (0.1%). Similarly, in the extracellular fraction the two main MCs were MC-LR
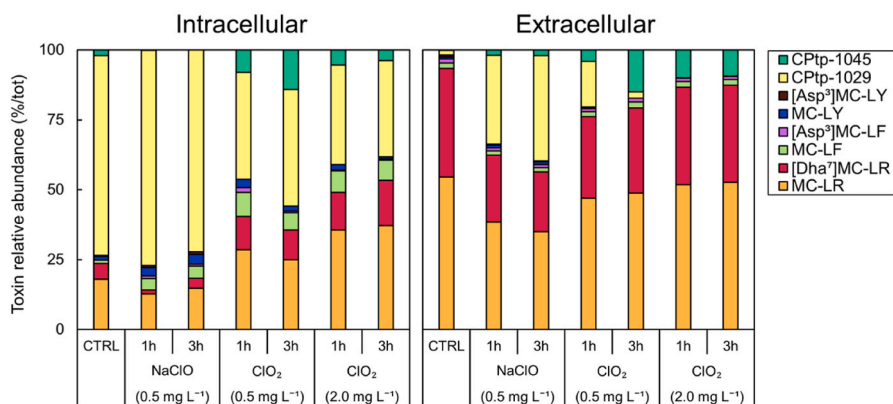
Fig. 3. Relative abundances of MCs variants and metabolites in *M. aeruginosa* cultures treated with NaClO and ClO$_2$ expressed as percentage on the total toxin content (μg L^{-1}) and divided for intracellular and extracellular fractions. CPtp-1029 = cyanopeptolin-type peptide-1029, CPtp-1045 = cyanopeptolin-type peptide-1045.

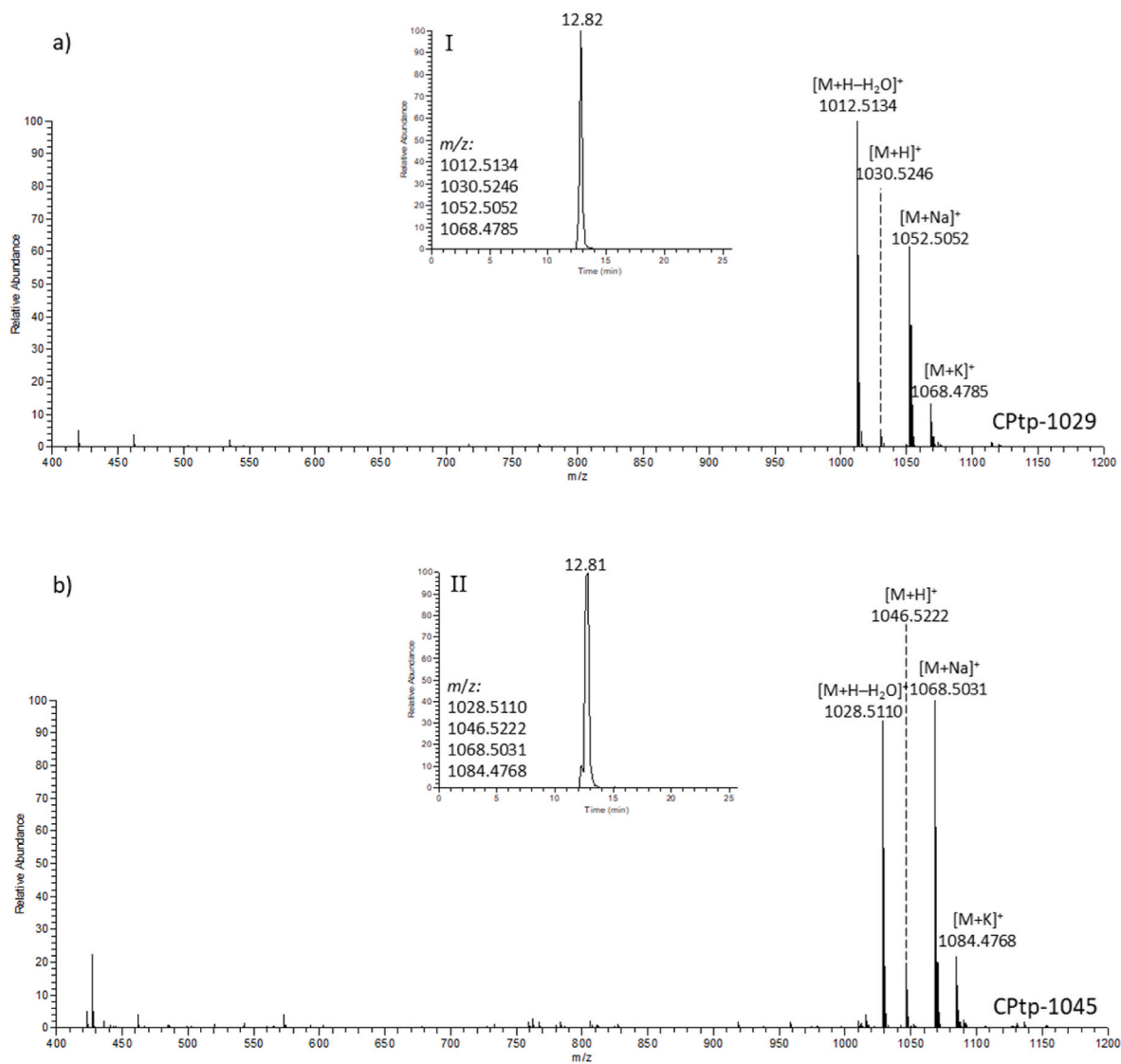**Fig. 4.** HR full-scan MS spectra of the new compound, a) cyanopeptolin-type peptide-1029 (CPtp-1029) in the control sample, and b) its oxidized analogue (CPtp-1045) in treated sample. Inset I: Extracted ion chromatogram (XIC) obtained by summing the [M+H]$^+$, [M+H–H$_2$O]$^+$, [M+Na]$^+$ and [M+K]$^+$ ions for CPtp-1029. Inset II: XIC obtained by summing the [M+H]$^+$, [M +H–H$_2$O]$^+$, [M+Na]$^+$ and [M+K]$^+$ ions for CPtp-1045.

and [Dha^7]MC-LR (Fig. 3, Table S4), nevertheless they were three- (54.6% vs 18.0%) and seven-fold (38.9% vs 5.7%) higher compared to the intracellular fraction, respectively. In samples subjected to both treatments, trace levels of MCs oxidized products (dihydroxy and monochloro-hydroxy MCs, Table S1) have been also detected. This suggested that chlorine treatments, at the low doses here tested (≤ 2 mg L^{-1}), only slightly promote MCs decomposition into the oxidized products. In addition to MCs, the untargeted LC-HRMS approach highlighted the presence in the analyzed samples of other cyanometabolites among which a particularly abundant new compound at m/z 1030.5246 eluting at 12.82 min was predominantly present in the biomass control sample (71.4%). The HR full scan MS spectrum (Fig. 4a) associated to the extracted ion chromatogram (XIC) of the ion at m/z 1030.5246 revealed the presence of a very intense *in-source* fragment due to the loss of a water molecule (at m/z 1012.5134), as well as [M+Na]$^+$ and [M+K]$^+$ adduct ions at m/z 1052.5052 and 1068.4785, respectively. The cross-checked interpretation of elemental formulae of all the protonated, *in-source* fragment, and adduct ions for the new compound, that we named cyanopeptolin-type peptide-1029 (CPtp-1029), allowed to assign it the elemental composition $C_{52}H_{71}O_{13}N_9$ (with the [M+H]$^+$ ion at m/z 1030.5246, $C_{52}H_{72}O_{13}N_9^+$ RDB = 21.5, Δ = 0.185 ppm). An oxidized derivative of CPtp-1029 at m/z 1046.5222 (Fig. 4b) was also identified as a minor constituent of *M. aeruginosa* biomass (2%, Fig. 3), whereas in the extracellular fraction it was present only in traces (0.1%). The assigned molecular formula, $C_{52}H_{71}O_{14}N_9$ (with the [M+H]$^+$ ion at m/z 1046.5222, $C_{52}H_{72}O_{14}N_9^+$ RDB = 21.5, Δ = 2.748 ppm), contained one O

atom more than CPtp-1029, likely a hydroxyl functionality, thus it was named cyanopeptolin-type peptide-1045 (CPtp-1045).

3.4. Multiple stage MS in structural characterization of the new cyanopeptolins

LC-HRMS^n (n = 2, 3) experiments were performed by fragmenting the main *in-source* [M+H–H$_2$O]$^+$ precursor ion at m/z 1012.5134 in both CID (Fig. S3a) and HCD (Fig. S4a) modes generating different, and complementary, diagnostic product ions (Table 1). The analysis of the CID HRMS^2 fragmentation pattern revealed the presence of a fragment at m/z 420.1914 corresponding to one of the conserved structural motif of CPtps ([Ahp^3+Phe^4+NMeTyr^5+H–H$_2$O]$^+$). An in-depth MS-based structural investigation provided for the identification of each single residue contained in the compound by observing diagnostic product ions (1–2 residues) in the HRMS^{2,3} spectra, including the neutral loss of individual residues from the precursor ion (Table 1). Successively, the cross-interpretation of oligopeptide product ions (3–5 residues) in the HRMS^{2,3} spectra allowed to infer the position of each residue in the cyclic structure (Figs. S3–S5). Particularly, the presence of NMeTyr, Choi, Phe and hydroxyPro residues was indicated by their immonium ions at m/z 150.0913 ($C_9H_{12}ON^+$, $\Delta = -0.270$ ppm), m/z 140.1069 ($C_8H_{14}ON^+$, $\Delta = -0.647$ ppm), m/z 120.0807 ($C_8H_{10}N^+$, $\Delta = -0.632$ ppm), and m/z 70.0649 ($C_4H_8N^+$, $\Delta = -3.223$ ppm), respectively. A Leu/Ile (indistinguishable based on MS evidence) was detected through the product ion at m/z 899.4313 ($C_{46}H_{59}O_{11}N_8^+$, $\Delta = +1.689$ ppm) due to the neutral loss of

Table 1
Assignment of product ions detected in CID and HCD spectra of cyanopeptolin-type peptide-1029 (CPtp-1029) precursor ion at m/z 1012.5 (see Figs. S3–S5).

	m/z	Formula	Sequence	Neutral loss
[M+H]$^+$	1030.5246	$C_{52}H_{72}O_{13}N_9^+$	[Choi^1+Gln^2+Ahp^3+Phe^4+NMeTyr^5+Leu/Ile^6+Hyp^7+Ala^8+H]$^+$	
[M+H–H$_2$O]$^+$	1012.5134	$C_{52}H_{70}O_{12}N_9^+$		H$_2$O
	995.4904	$C_{52}H_{67}O_{12}N_8^+$		H$_2$O+NH$_3$
	994.5020	$C_{52}H_{68}O_{11}N_9^+$		2H$_2$O

	m/z	Formula	Sequence	Neutral loss
CID	899.4313	$C_{46}H_{59}O_{11}N_8^+$	[Hyp^7+Ala^8+Choi^1+Gln^2+Ahp^3+Phe^4+NMeTyr^5+H–H$_2$O]$^+$	Leu/Ile^6+H$_2$O
	881.4190	$C_{46}H_{57}O_{10}N_8^+$	[Hyp^7+Ala^8+Choi^1+Gln^2+Ahp^3+Phe^4+NMeTyr^5+H–2H$_2$O]$^+$	Leu/Ile^6+2H$_2$O
	770.4078	$C_{38}H_{56}O_{10}N_7^+$	[Gln^2+ Choi^1+Ala^8+Hyp^7+Leu/Ile^6+NMeTyr^5+H]$^+$	Ahp^3+Phe^4
	752.3974	$C_{38}H_{54}O_9N_7^+$	[Gln^2+ Choi^1+Ala^8+Hyp^7+Leu/Ile^6+NMeTyr^5+H–H$_2$O]$^+$	Ahp^3+Phe^4+H$_2$O
	717.3604	$C_{38}H_{49}O_8N_6^+$	[Choi^1+Gln^2+Ahp^3+Phe^4+NMeTyr^5+H–H$_2$O]$^+$	Leu/Ile^6+Hyp^7+Ala^8+H$_2$O
	699.3492[b]	$C_{38}H_{47}O_7N_6^+$	[Choi^1+Gln^2+Ahp^3+Phe^4+NMeTyr^5+H–2H$_2$O]$^+$	Leu/Ile^6+Hyp^7+Ala^8+2H$_2$O
	593.3287	$C_{28}H_{45}O_8N_6^+$	[Gln^2+ Choi^1+Ala^8+Hyp^7+Leu/Ile^6+H–H$_2$O]$^+$	Ahp^3+Phe^4+NMeTyr^5+H$_2$O
	503.2283	$C_{28}H_{31}O_5N_4^+$	[Gln^2+Ahp^3+Phe^4+NMeTyr^5+H–CO–NH$_2$–H$_2$O]$^+$	Leu/Ile^6+Hyp^7+Ala^8+ Choi^1+CO+NH$_2$+H$_2$O
	462.2343[a]	$C_{22}H_{32}O_6N_5^+$	[Gln^2+ Choi^1+Ala^8+Hyp^7+H]$^+$	Ahp^3+Phe^4+NMeTyr^5+Leu/Ile^6
	420.1914[b]	$C_{24}H_{26}O_4N_3^+$	[Ahp^3+Phe^4+NMeTyr^5+H–H$_2$O]$^+$	Choi^1+Gln^2+Leu/Ile^6+Hyp^7+Ala^8+H$_2$O
	296.1600[a,c]	$C_{14}H_{22}O_4N_3^+$	[Choi^1+Gln^2+H]$^+$	Ahp^3+Phe^4+NMeTyr^5+Leu/Ile^6+Hyp^7+Ala^8
HCD	308.1281	$C_{19}H_{18}O_3N^+$	[Phe^4+NMeTyr^5+H–H$_2$O]$^+$	Choi^1+Gln^2+Ahp^3+Leu/Ile^6+Hyp^7+Ala^8+H$_2$O
	243.1129	$C_{14}H_{15}O_2N_2^+$	[Ahp^3+Phe^4+H–H$_2$O]$^+$	Choi^1+Gln^2+NMeTyr^5+Leu/Ile^6+Hyp^7+Ala^8+H$_2$O
	215.1179	$C_{13}H_{15}ON_2^+$	[Ahp^3+Phe^4+H–CO–H$_2$O]$^+$	Choi^1+Gln^2+NMeTyr^5+Leu/Ile^6+Hyp^7+Ala^8+CO+H$_2$O
	187.1230	$C_{12}H_{15}N_2^+$	[Ahp^3+Phe^4+H–2CO–H$_2$O]$^+$	Choi^1+Gln^2+NMeTyr^5+Leu/Ile^6+Hyp^7+Ala^8+2CO+H$_2$O
	168.1019[c]	$C_9H_{14}O_2N^+$	[Choi^1 (immonium ion)+CO+H]$^+$	Gln^2+Ahp^3+Phe^4+NMeTyr^5+Leu/Ile^6+Hyp^7+Ala^8
	150.0913	$C_9H_{12}ON^+$	[NMeTyr^5+H]$^+$	Choi^1+Gln^2+Ahp^3+Leu/Ile^6+Hyp^7+Ala^8
	140.1069[c]	$C_8H_{14}ON^+$	[Choi^1(immonium ion)+H]$^+$	Gln^2+Ahp^3+Phe^4+NMeTyr^5+Leu/Ile^6+Hyp^7+Ala^8
	120.0807	$C_8H_{10}N^+$	[Phe^4(immonium ion)+H]$^+$	Choi^1+Gln^2+Ahp^3+NMeTyr^5+Leu/Ile^6+Hyp^7+Ala^8
	70.0649	$C_4H_8N^+$	[Hyp^7(immonium ion)+H]$^+$	Choi^1+Gln^2+Ahp^3+Phe^4+NMeTyr^5+Leu/Ile^6+Ala^8

[a]Fragment confirmed also in LC-HRMS^3 experiment, precursor ion at m/z 770.4078; [b]Fragment confirmed also in LC-HRMS^3 experiment, precursor ion at m/z 717.3604; [c]Fragment confirmed also in LC-HRMS^3 experiment, precursor ion at m/z 462.2343.

$C_6H_{11}ON$ (113.0821 Da) from the precursor ion. Product ions at m/z 243.1129 ($C_{14}H_{15}O_2N_2^+$, $\Delta = +0.394$) and 215.1179 ($C_{13}H_{15}ON_2^+$, $\Delta = +0.048$ ppm) indicated the sequence Ahp+Phe as well as the fragment ion at m/z 296.1600 ($C_{14}H_{22}O_4N_3^+$ $\Delta = -1.630$ ppm) revealed the sequence Choi+Gln. The presence of the characteristic product ion at m/z 420.1914 pointing out the sequence Ahp[3]+Phe[4]+NMeTyr[5] in combination with a fragment ion at m/z 717.3604, corresponding to the sequence [Choi[1]+Gln[2]+Ahp[3]+Phe[4]+NMeTyr[5]+H–H_2O]$^+$ allowed to locate Choi[1]+Gln[2]. A Leu/Ile at position-6, a HydroxyPro[7] and Ala[8] were suggested by: i) a product ion at m/z 770.4078 corresponding to [Gln[2]+Choi[1]+Ala[8]+Hyp[7]+Leu/Ile[6]+NMeTyr[5]+H]$^+$ and ii) a product ion at m/z 462.2343 corresponding to the neutral loss of Ahp[3]+-Phe[4]+NMeTyr[5]+Leu/Ile[6] from the precursor ion (Table 1). HRMS[3] experiments carried out by further fragmenting the main product ions at m/z 770.4078, 462.2343, 717.3604 (Fig. S5, Table 1) provided additional evidence of the amino acids sequence. As for CPtp-1045, HRMS[2] spectrum showed a fragment at m/z 166.0866 versus the fragment at m/z 150.0913 obtained for CPtp-1029 suggesting a *N*-methyl hydroxy Tyr (versus *N*-methyl Tyr) at position-5 (Fig. S4b, Table S5).

3.5. Content variation of microcystins and of cyanopeptolin-type peptides

Toxin content in *M. aeruginosa* cultures after the addition of each chlorinated oxidant and the resulting percent variation compared to controls (ΔTox(%)) is reported in Fig. 5. Despite having similar relative abundances (Fig. 3), it was observed that MCs levels were markedly higher in the extracellular fraction than in the biomass following the treatments regardless of the oxidant used, the dose and the treatment time (Fig. 5a.; Table S4; ANOVA, p < 0.05). The percent variation of intracellular toxins between controls and ClO_2-treated cultures was significantly higher compared to NaClO-treated cultures, being 99 vs 93%, respectively (Fig. 5b.; ANOVA, $p < 0.05$). Nonetheless, the simultaneous increase of extracellular toxins released in water was

Fig. 5. Toxins' content in *M. aeruginosa* cultures (n = 3) treated with ClO_2 and NaClO and percent variation of their content compared to controls in each fraction, measured by LC-HRMS, i.e., intracellular (filled columns) and extracellular (striped columns); a) toxin content per volume (μg L^{-1}) and b) relative percent variation ΔTox(%). Significant differences compared to a) control and b) among treatments are indicated with asterisks (ANOVA, $p < 0.05$).

observed for treated cultures compared to controls. Specifically, a two-fold increase for NaClO-treated cultures was observed (Fig. 5a; ANOVA, $p < 0.05$), whereas for ClO_2 no significant effects were reported at the same low dose (0.5 mg L^{-1}, ANOVA, $p > 0.05$). Only the highest dose of ClO_2 led to a decrease in extracellular toxin contents, which resulted in the actual effective treatment for the toxins removal (Fig. 5b; ΔTox 18–21%, ANOVA, $p < 0.05$). As for total toxin content (intracellular plus extracellular fractions), the concentration was significantly reduced compared to the controls only for cultures treated with the highest dose of ClO_2, regardless of the treatment time (Table S4; ANOVA, $p < 0.05$). When comparing the concentrations of toxins expressed per liter to those per number of cells (Table S4), their relative abundances were similar (Fig. 3 vs Fig. S6). Only minor differences were reported and were due to the reduced cell density in ClO_2-treated samples (Fig. 2a).

Unlike the MCs, CPtp-1029 was retained inside the cells (81 vs 2 μg L^{-1}, Table S4) being the main compound of the intracellular fraction (71.4%, Fig. 3). The percent variation of each toxin and CPtps between controls and each treatment for the intracellular and extracellular fractions, i.e., ΔTox(%), is reported in Fig. 6. Regardless of the treatment used, both MC variants and the new CPtp-1029 were removed from the cells, although the extent of the removal was generally higher for ClO_2-than NaClO-treated cultures, especially for MC-LY and MC-LF and their [Asp[3]]-analogues (Fig. 6). CPtp-1029 was particularly affected by all treatments, both in intracellular and extracellular fractions, turning into its oxidized derivative (Fig. 3). In NaClO-treated cultures, CPtp-1029 accounted for 72–76% of *M. aeruginosa* intracellular fraction profile, whereas in ClO_2-treated cultures its relative intracellular abundance decreased to 33–41% (Fig. 3). In extracellular fractions, CPtp-1029 concentration increased following oxidant treatments compared to the controls, especially when using NaClO (2 vs 80–100 μg L^{-1}, respectively, Table S4). Thus, the percent variation of CPtp-1029 content resulted negative and about -100% for NaClO treatment compared to controls (Fig. 6). The overall results suggest that CPtp-1029 was not degraded in the biomass by NaClO but released in water likely as a consequence of cell damage, hence accounting for 32–37% of the extracellular fraction (Fig. 3). Conversely, in ClO_2-treated cultures, the relative abundance of CPtp-1029 in extracellular fraction decreased to 19% after 1 h of treatment at the lowest dose (0.5 mg L^{-1}), whereas dropped to near 1% in all the other conditions (Fig. 3). The actual removal of CPtp-1029 from water was only achieved at the highest ClO_2 dose (ΔTox 85–93%, Fig. 6). A simultaneous increase in the abundance of the oxidized derivative, CPtp-1045, was observed in the extracellular fraction, especially after the addition of ClO_2. This effect was particularly evident when comparing the residual extracellular concentration of the two CPtps following the treatment with ClO_2 at the lowest dose (Fig. 3, Table S4); after 1 h, CPtp-1029 was still present in relatively high amounts and CPtp-1045 was less abundant (31 and 8 μg L^{-1}, respectively). After 3 h an opposite trend emerged, as the concentration of the CPtp-1029 drastically decreased while its oxidized derivative increased (4 and 27 μg L^{-1}, respectively).

4. Discussion

The use of both oxidants, ClO_2 and NaClO, led to the inhibition of the photosynthetic activity of *M. aeruginosa*, in agreement with previous observations (Li et al., 2020; Zhou et al., 2014). The results obtained herein showed how NaClO affected cell viability at markedly lower doses compared to ClO_2 (0.5 vs 0.8 mg L^{-1}). While ClO_2 remains as a dissolved gas in the solution when added to water, NaClO dissociates forming HClO, that can permeate the negatively charged cyanobacterial cells, causing damage at the membrane and intracellular levels (Li et al., 2018). Additionally, at the tested doses, chosen in the range of EC_{50} values (i.e., 0.4–0.6 mg L^{-1} for ClO_2 and 0.3–0.4 mg L^{-1} for NaClO), the photosynthetic activity of *M. aeruginosa* firstly decreased following short-term treatment of 1 h, but slightly increased after 24 h. This
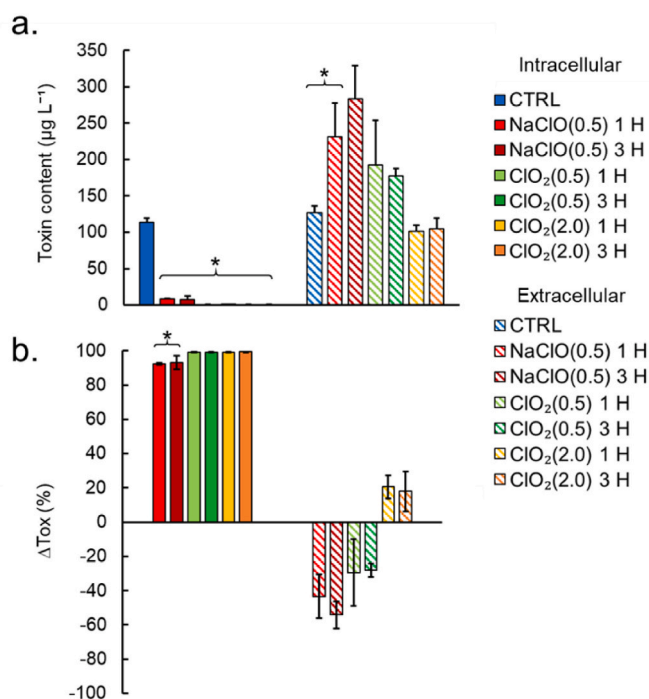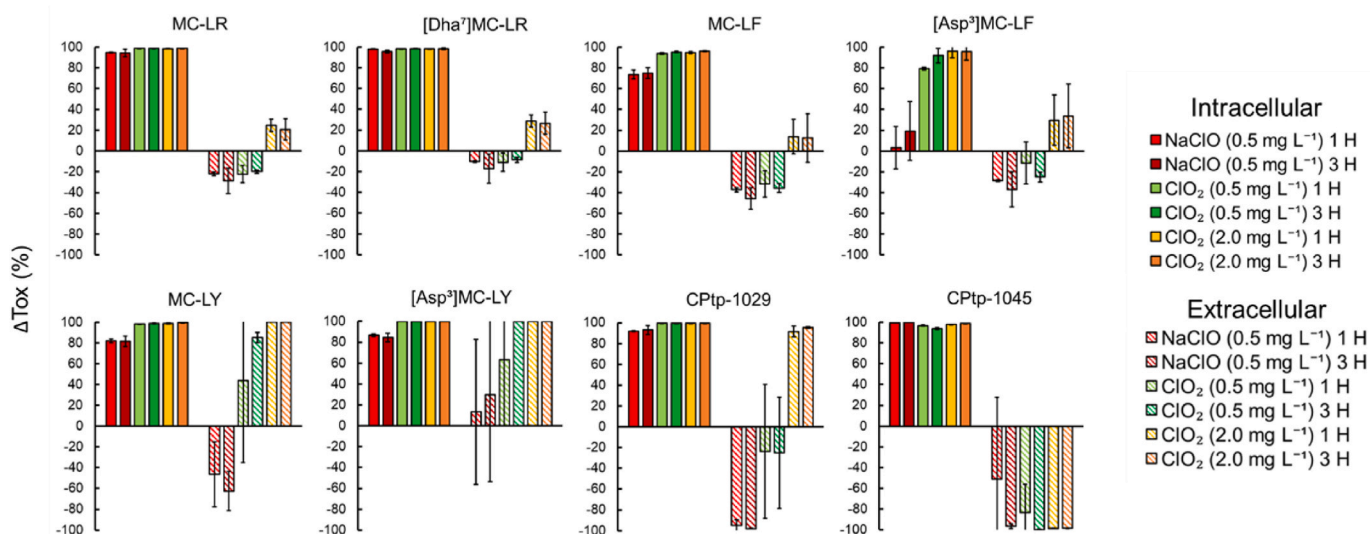
Fig. 6. Percent variation of each toxin variants (ΔTox(%)) after oxidation treatments with NaClO and ClO$_2$ in intracellular (filled columns) and extracellular (striped columns) fractions based on toxin concentrations per volume (μg L^{-1}).

evidence may indicate that the cultures treated with low doses of both oxidants were likely experiencing a temporary stress, rather than structural damages, since treated cells were able to partially recover their photosynthetic capacity after 1 day. In cyanobacteria, low values of both maximum and effective quantum yield in the range 0.00–0.05 (corresponding to 0–20% photosynthetic activity compared to controls) are usually reported for moderately-to-severely damaged cyanobacteria cells (Mikula et al., 2012; Singh et al., 2024). While overdosing with oxidants (>2 mg L^{-1}) may lead to various issues, including the formation of DBPs, increase of turbidity and dissolved organic carbon, toxin and taste-and-odour compounds release (Henderson et al., 2008; Jalili et al., 2022; Qi et al., 2021), soft-chlorination could shift the community composition in natural assemblages leading to the persistence of some species less-susceptible to the oxidation (Moradinejad et al., 2020). Other studies have investigated how chlorinated oxidants differently affect cyanobacteria (i.e., cellular integrity, cells density, viability, toxin content), both in cultures (Ding et al., 2010; Fan et al., 2013; Li et al., 2020; Moradinejad et al., 2019; Wert et al., 2014; Zamyadi et al., 2013; Zhou et al., 2014) and natural-occurring blooms (Greenstein et al., 2020; He and Wert, 2016; Ye et al., 2019), emphasizing how different test conditions and organisms can be differently affected by the treatments. It is noteworthy that the present study was conducted on a cultured strain of *M. aeruginosa*, consisting of single cells not aggregated in a colonial form, a common outcome observed under culture conditions (Le et al., 2022). In natural environment, however, *Microcystis* spp. tends to form spherical-to-irregular colonies associated with extracellular polysaccharides and microbiota, which could influence the effects here reported. The release of intracellular toxins into water and the simultaneous increase of their extracellular concentration were previously observed (He and Wert, 2016; Li et al., 2020; Wert et al., 2014; Zhang et al., 2017), suggesting that the rate of toxin degradation into nontoxic dihydroxy or monochloro-hydroxy derivatives (Kull et al., 2004), could be slower than its release due to oxidation-driven cellular damage (Ding et al., 2010; Fan et al., 2013). Although noxious DBPs - collectively known as trihalomethanes and haloacetic acids - are outside the scope of this study, evidence exists that water chlorination using NaClO may lead to their formation because of reaction with natural organic matter (Mazhar et al., 2020). Using ClO$_2$ is generally considered safer than other chlorinated oxidants because it does not form trihalomethanes, but in alkaline conditions it may react with OH$^-$ in solution to form ClO$_2^-$ and ClO$_3^-$, or other DBPs of health concerns whose formation depletes ClO$_2$ for oxidation of cyanotoxins (Sorlini et al., 2014). Therefore,

although better results in toxin removal were here obtained when using the highest dose of ClO$_2$ (2.0 mg L^{-1}), overdosing should be further discouraged. Additionally, the low concentrations of MCs oxidized products found in the present study agreed with the results by Kull et al. (2004) describing the effective oxidation of MCs occurring only at high ClO$_2$ concentrations (107 mg L^{-1}).

Oxidation may act differently on each MC variant depending both on the amino acid residues and operational conditions (He et al., 2017). The reactivity of free chlorine is expected to be lower for MCs containing relatively unreactive aliphatic amino acids (e.g., MC-LA containing both leucine and alanine), and higher for those variants having amino acids with aromatic rings (e.g., MC-YR). Similarly, during the here-set oxidation experiment, the major removal effect was observed for MC-LY and MC-LF variants, each containing amino acids with an aromatic ring (Y = tyrosine, F = phenylalanine). Most of the studies regarding MCs are focused on MC-LR, which is well characterized for its toxicity, whereas little is known about other minority variants. Among them, MC-LF has been proven to be more toxic compared to MC-LR towards different cell lines, likely due to its greater hydrophobicity characteristics. Additionally, synergic effects of MCs mixture are still not well understood, but should not be neglected considering that MCs-producing cyanobacteria usually synthetize a plethora of them in natural environment (Díez-Quijada et al., 2019). To the best of our knowledge, no studies on the effects of chlorinated oxidants on cyanopeptolin-type peptides have been conducted so far, whose presence as major components have emerged thanks to the untargeted LC-HRMS approach here used. While the potential ecotoxicity of CPtps has still not been investigated, toxic effects of purified extracts of similar metabolites (i.e., cyanopeptolins) have emerged when tested on model organisms; for instance reduced reproduction and lifespan, together with affected valvular integrity was observed in the nematode *Caenorhabditis elegans* (Lenz et al., 2019), whereas neurotoxic effects have emerged in zebrafish embryos (Faltermann et al., 2014). Noteworthy, cyanopeptolins and MCs concentrations found in freshwaters are often comparable (Beversdorf et al., 2017). Most of the epidemiological studies on cyanotoxins focused on the potential exposure to well-known MCs, while the inclusion of less studied cyanobacterial peptides, such as CPtps, could give new insights especially when observing symptoms not ascribable to the presence of other known toxins (Janssen, 2019). Furthermore, potential risks associated with the co-occurrence of multiple cyanometabolite classes may boost a synergistic toxic effect that has not been investigated so far. Thus, the implementation of untargeted

LC-HRMS methods able to investigate the whole cyanometabolite profile appears desirable to guarantee human and animal safety.

5. Conclusions

The chlorinated oxidants NaClO and ClO_2 were able to inactivate *M. aeruginosa* cells at a low dose of 0.5 mg L^{-1}. High toxin removal from cyanobacterial cells and simultaneous increase in water was observed for both oxidants, suggesting possible cell damage, while a longer treatment time resulted not effective. While ClO_2 degraded cyanobacterial cells and total toxins, NaClO possibly stimulated the extracellular toxin release, without an effective removal. Untargeted LC-HRMS led to identify two new cyanopeptolin-type peptides, CPtp-1029 and its oxidation derivative, CPtp-1045, with the latter increasing in extracellular fraction after oxidation treatment, especially when using ClO_2. These findings suggest that the toxicological risks associated with the presence of CPtps in the pre-oxidized drinking water should not be neglected. The choice of the oxidant to be used during raw water pre-treatment for potabilization purposes, as well as its dose and treatment time, should be taken into consideration. Since the success of a specific treatment highly depends on several environmental conditions (e.g., pH, temperature, organic matter), it is difficult to establish what the best pre-oxidation practice might be. The use of lower (<2 mg L^{-1}) oxidant doses may limit treatment costs, while maintaining the benefits of using pre-oxidation before subsequent downstream potabilization processes. Finally, major efforts should be put into understanding the fate of such compounds at downstream processes in DWTPs and their potential presence in finished water.

CRediT authorship contribution statement

Mara Simonazzi: Writing – original draft, Visualization, Investigation, Formal analysis, Conceptualization. **Antonella Miglione:** Writing – review & editing, Visualization, Investigation. **Luciana Tartaglione:** Writing – review & editing, Supervision, Methodology, Investigation, Funding acquisition, Data curation. **Michela Varra:** Writing – review & editing, Investigation. **Carmela DellAversano:** Writing – review & editing, Project administration. **Franca Guerrini:** Writing – review & editing, Investigation. **Rossella Pistocchi:** Writing – review & editing, Supervision, Project administration, Funding acquisition, Conceptualization. **Laura Pezzolesi:** Writing – review & editing, Supervision, Methodology, Investigation, Conceptualization.

Declaration of competing interest

The authors declare that they have no known competing financial interests or personal relationships that could have appeared to influence the work reported in this paper.

Data availability

Data will be made available on request.

Appendix A. Supplementary data

Supplementary data to this article can be found online at https://doi.org/10.1016/j.chemosphere.2024.142976.

References

Betancourt, W.Q., Rose, J.B., 2004. Drinking water treatment processes for removal of *Cryptosporidium* and *Giardia*. Vet. Parasitol. https://doi.org/10.1016/j.vetpar.2004.09.002.

Beversdorf, L.J., Weirich, C.A., Bartlett, S.L., Miller, T.R., 2017. Variable cyanobacterial toxin and metabolite profiles across six eutrophic lakes of differing physiochemical characteristics. Toxins. https://doi.org/10.3390/toxins9020062.

Buratti, F.M., Manganelli, M., Vichi, S., Stefanelli, M., Scardala, S., Testai, E., Funari, E., 2017. Cyanotoxins: producing organisms, occurrence, toxicity, mechanism of action and human health toxicological risk evaluation. Arch. Toxicol. 91, 1049–1130. https://doi.org/10.1007/s00204-016-1913-6.

Christophoridis, C., Zervou, S.K., Manolidi, K., Katsiapi, M., Moustaka-Gouni, M., Kaloudis, T., Triantis, T.M., Hiskia, A., 2018. Occurrence and diversity of cyanotoxins in Greek lakes. Sci. Rep. https://doi.org/10.1038/s41598-018-35428-x.

de la Cruz, A.A., Chernoff, N., Sinclair, J.L., Hill, D., Diggs, D.L., Lynch, A.T., 2020. Introduction to cyanobacteria and cyanotoxins. In: Water Treatment for Purification from Cyanobacteria and Cyanotoxins, pp. 1–35. https://doi.org/10.1002/9781118928677.ch1.

Díez-Quijada, L., Prieto, A.I., Guzmán-Guillén, R., Jos, A., Cameán, A.M., 2019. Occurrence and toxicity of microcystin congeners other than MC-LR and MC-RR: a review. Food Chem. Toxicol. 125, 106–132. https://doi.org/10.1016/j.fct.2018.12.042.

Ding, J., Shi, H., Timmons, T., Adams, C., 2010. Release and removal of microcystins from *Microcystis* during oxidative-, physical-, and UV-based disinfection. J. Environ. Eng. 136, 2–11. https://doi.org/10.1061/(asce)ee.1943-7870.0000114.

Faltermann, S., Zucchi, S., Kohler, E., Blom, J.F., Pernthaler, J., Fent, K., 2014. Molecular effects of the cyanobacterial toxin cyanopeptolin (CP1020) occurring in algal blooms: global transcriptome analysis in zebrafish embryos. Aquat. Toxicol. https://doi.org/10.1016/j.aquatox.2014.01.018.

Fan, J., Ho, L., Hobson, P., Brookes, J., 2013. Evaluating the effectiveness of copper sulphate, chlorine, potassium permanganate, hydrogen peroxide and ozone on cyanobacterial cell integrity. Water Res. https://doi.org/10.1016/j.watres.2013.05.057.

Fastner, J., Humpage, A., 2021. Cyanobacterial toxins. In: Chorus, I., Welker, M. (Eds.), Toxic Cyanobacteria in Water: A Guide to Their Public Health Consequences, Monitoring and Management. CRC Press, pp. 13–162. https://doi.org/10.1515/9783110442045-007.

Greenstein, K.E., Zamyadi, A., Glover, C.M., Adams, C., Rosenfeldt, E., Wert, E.C., 2020. Delayed release of intracellular microcystin following partial oxidation of cultured and naturally occurring cyanobacteria. Toxins 12, 1–16. https://doi.org/10.3390/toxins12050335.

Hammer, Ø., Harper, D.A.T.a.T., Ryan, P.D., 2001. PAST: paleontological statistics software package for education and data analysis. Palaeontol. Electron. 4, 1–9. https://doi.org/10.1016/j.bcp.2008.05.025.

He, X., Stanford, B.D., Adams, C., Rosenfeldt, E.J., Wert, E.C., 2017. Varied influence of microcystin structural difference on ELISA cross-reactivity and chlorination efficiency of congener mixtures. Water Res. 126, 515–523. https://doi.org/10.1016/j.watres.2017.09.037.

He, X., Wert, E.C., 2016. Colonial cell disaggregation and intracellular microcystin release following chlorination of naturally occurring *Microcystis*. Water Res. 101, 10–16. https://doi.org/10.1016/j.watres.2016.05.057.

Henderson, R., Parsons, S.A., Jefferson, B., 2008. The impact of algal properties and pre-oxidation on solid-liquid separation of algae. Water Res. 42, 1827–1845. https://doi.org/10.1016/j.watres.2007.11.039.

Huisman, J., Codd, G.A., Paerl, H.W., Ibelings, B.W., Verspagen, J.M.H., Visser, P.M., 2018. Cyanobacterial blooms. Nat. Rev. Microbiol. 16, 471–483. https://doi.org/10.1038/s41579-018-0040-1.

Italian Legislative Decree 152/2006, 2006. Italian Legislative Decree (152/2006). Norme Mater. Ambient. (G.U. n. 88 del 14 April).

Jalili, F., Moradinejad, S., Zamyadi, A., Dorner, S., Sauvé, S., Prévost, M., 2022. Evidence-based framework to manage cyanobacteria and cyanotoxins in water and sludge from drinking water treatment plants. Toxins 14. https://doi.org/10.3390/toxins14060410.

Janssen, E.M.-L., Jones, M.R., Pinto, E., Dörr, F., Torres, M.A., Rios Jacinavicius, F., Mazur-Marzec, H., Szubert, K., Konkel, R., Tartaglione, L., Dell'Aversano, C., Miglione, A., McCarron, P., Beach, D.G., Miles, C.O., Fewer, D.P., Sivonen, K., Jokela, J., Wahlsten, M., Niedermeyer, T.H.J., Schanbacher, F., Leão, P., Preto, M., D'Agostino, P.M., Baunach, M., Dittmann, E., Reher, R., 2023. S75 | CyanoMetDB | Comprehensive database of secondary metabolites from cyanobacteria (NORMAN-SLE-S75.0.2.0). Zenodo. https://doi.org/10.5281/zenodo.7922070 [Data set].

Janssen, E.M.L., 2019. Cyanobacterial peptides beyond microcystins – a review on co-occurrence, toxicity, and challenges for risk assessment. Water Res. 151, 488–499. https://doi.org/10.1016/j.watres.2018.12.048.

Jones, M.R., Pinto, E., Torres, M.A., Dörr, F., Mazur-Marzec, H., Szubert, K., Tartaglione, L., Dell'Aversano, C., Miles, C.O., Beach, D.G., McCarron, P., Sivonen, K., Fewer, D.P., Jokela, J., Janssen, E.M.L., 2021. CyanoMetDB, a comprehensive public database of secondary metabolites from cyanobacteria. Water Res. 196, 117017 https://doi.org/10.1016/j.watres.2021.117017.

Kaloudis, T., Zervou, S.K., Tsimeli, K., Triantis, T.M., Fotiou, T., Hiskia, A., 2013. Determination of microcystins and nodularin (cyanobacterial toxins) in water by LC-MS/MS. Monitoring of Lake Marathonas, a water reservoir of Athens, Greece. J. Hazard Mater. 263, 105–115. https://doi.org/10.1016/j.jhazmat.2013.07.036.

Konkel, R., Cegłowska, M., Szubert, K., Wieczerzak, E., Iliakopoulou, S., Kaloudis, T., Mazur-Marzec, H., 2023. Structural diversity and biological activity of cyanopeptolins produced by *Nostoc edaphicum* CCNP1411. Mar. Drugs 21, 508.

Kull, T.P.J., Backlund, P.H., Karlsson, K.M., Meriluoto, J.A.O., 2004. Oxidation of the cyanobacterial hepatotoxin microcystin-LR by chlorine dioxide: reaction kinetics, characterization, and toxicity of reaction products. Environ. Sci. Technol. 38, 6025–6031. https://doi.org/10.1021/es0400032.

Kust, A., Řeháková, K., Vrba, J., Maicher, V., Mareš, J., Hrouzek, P., Chiriac, M.C., Benedová, Z., Tesařová, B., Saurav, K., 2020. Insight into unprecedented diversity of cyanopeptides in eutrophic ponds using an MS/MS networking approach. Toxins. https://doi.org/10.3390/toxins12090561.

Le, V. Van, Srivastava, A., Ko, S.R., Ahn, C.Y., Oh, H.M., 2022. *Microcystis* colony formation: extracellular polymeric substance, associated microorganisms, and its application. Bioresour. Technol. 360, 127610 https://doi.org/10.1016/j.biortech.2022.127610.

Lenz, K.A., Miller, T.R., Ma, H., 2019. Anabaenopeptins and cyanopeptolins induce systemic toxicity effects in a model organism the nematode *Caenorhabditis elegans*. Chemosphere 214, 60–69. https://doi.org/10.1016/j.chemosphere.2018.09.076.

Li, L., Zhu, C., Xie, C., Shao, C., Yu, S., Zhao, L., Gao, N., 2018. Kinetics and mechanism of *Pseudoanabaena* cell inactivation, 2-MIB release and degradation under exposure of ozone, chlorine and permanganate. Water Res. 147, 422–428. https://doi.org/10.1016/j.watres.2018.10.023.

Li, X., Chen, S., Zeng, J., Song, W., Yu, X., 2020. Comparing the effects of chlorination on membrane integrity and toxin fate of high- and low-viability cyanobacteria. Water Res. 177 https://doi.org/10.1016/j.watres.2020.115769.

Mazhar, M.A., Khan, N.A., Ahmed, S., Khan, A.H., Hussain, A., Rahisuddin, Changani, F., Yousefi, M., Ahmadi, S., Vambol, V., 2020. Chlorination disinfection by-products in municipal drinking water – a review. J. Clean. Prod. https://doi.org/10.1016/j.jclepro.2020.123159.

McDonald, K., Renaud, J.B., Pick, F.R., Miller, J.D., Sumarah, M.W., McMullin, D.R., 2021. Diagnostic fragmentation filtering for cyanopeptolin detection. Environ. Toxicol. Chem. https://doi.org/10.1002/etc.4941.

Mikula, P., Zezulka, S., Jancula, D., Marsalek, B., 2012. Metabolic activity and membrane integrity changes in *Microcystis aeruginosa* - new findings on hydrogen peroxide toxicity in cyanobacteria. Eur. J. Phycol. 47, 195–206. https://doi.org/10.1080/09670262.2012.687144.

Mohamed, Z.A., 2016. Breakthrough of *Oscillatoria limnetica* and microcystin toxins into drinking water treatment plants – examples from the Nile River, Egypt. WaterSA 42, 161–165. https://doi.org/10.4314/wsa.v42i1.16.

Moradinejad, S., Glover, C.M., Mailly, J., Seighalani, T.Z., Peldszus, S., Barbeau, B., Dorner, S., Prévost, M., Zamyadi, A., 2019. Using advanced spectroscopy and organic matter characterization to evaluate the impact of oxidation on cyanobacteria. Toxins 11. https://doi.org/10.3390/toxins11050278.

Moradinejad, S., Trigui, H., Maldonado, J.F.G., Shapiro, J., Terrat, Y., Zamyadi, A., Dorner, S., Prévost, M., 2020. Diversity assessment of toxic cyanobacterial blooms during oxidation. Toxins. https://doi.org/10.3390/toxins12110728.

Moreira, C., Vasconcelos, V., Antunes, A., 2022. Cyanobacterial blooms: current knowledge and new perspectives. Earth 3, 127–135. https://doi.org/10.3390/earth3010010.

Pazouki, P., Prévost, M., McQuaid, N., Barbeau, B., de Boutray, M.L., Zamyadi, A., Dorner, S., 2016. Breakthrough of cyanobacteria in bank filtration. Water Res. https://doi.org/10.1016/j.watres.2016.06.037.

Pestana, C.J., Reeve, P.J., Sawade, E., Voldoire, C.F., Newton, K., Praptiwi, R., Collingnon, L., Dreyfus, J., Hobson, P., Gaget, V., Newcombe, G., 2016. Fate of cyanobacteria in drinking water treatment plant lagoon supernatant and sludge. Sci. Total Environ. https://doi.org/10.1016/j.scitotenv.2016.05.173.

Pichierri, S., Pezzolesi, L., Vanucci, S., Totti, C., Pistocchi, R., 2016. Inhibitory effect of polyunsaturated aldehydes (PUAs) on the growth of the toxic benthic dinoflagellate Ostreopsis cf. ovata. Aquat. Toxicol. 179, 125–133. https://doi.org/10.1016/j.aquatox.2016.08.018.

Qi, J., Ma, B., Miao, S., Liu, R., Hu, C., Qu, J., 2021. Pre-oxidation enhanced cyanobacteria removal in drinking water treatment: a review. J. Environ. Sci. 110, 160–168. https://doi.org/10.1016/j.jes.2021.03.040.

R Core Team, 2022. R: A Language and Environment for Statistical Computing. R Found. Stat. Comput, Vienna, Austria, 2022. R Core Team.

Rose, A.K., Fabbro, L., Kinnear, S., 2018. Cyanobacteria breakthrough: effects of *Limnothrix redekei* contamination in an artificial bank filtration on a regional water supply. Harmful Algae 76, 1–10. https://doi.org/10.1016/j.hal.2018.04.010.

Singh, P.R., Gupta, A., Singh, A.P., Jaiswal, J., Sinha, R.P., 2024. Effects of ultraviolet radiation on cellular functions of the cyanobacterium *Synechocystis* sp. PCC 6803 and its recovery under photosynthetically active radiation. J. Photochem. Photobiol. B Biol. 252, 112866 https://doi.org/10.1016/j.jphotobiol.2024.112866.

Sorlini, S., Gialdini, F., Biasibetti, M., Collivignarelli, C., 2014. Influence of drinking water treatments on chlorine dioxide consumption and chlorite/chlorate formation. Water Res. 54, 44–52. https://doi.org/10.1016/j.watres.2014.01.038.

Stanier, R.Y., Kunisawa, R., Mandel, M., Cohen-Bazire, G., 1971. Purification and properties of unicellular blue-green algae (order Chroococcales). Bacteriol. Rev. 35, 171–205. https://doi.org/10.1128/br.35.2.171-205.1971.

Utermöhl, H., 1931. Neue Wege in der quantitativen Erfassung des Plankton (mit besonderer Berücksichtigung des Ultraplanktons.). Verhandlungen der Int. Vereinigung für Theor. und Angew. Limnol. 5, 567–596. https://doi.org/10.1080/03680770.1931.11898492.

Varriale, F., Tartaglione, L., Zervou, S.-K., Miles, C.O., Mazur-Marzec, H., Triantis, T.M., Kaloudis, T., Hiskia, A., Dell'Aversano, C., 2023. Untargeted and targeted LC-MS and data processing workflow for the comprehensive analysis of oligopeptides from cyanobacteria. Chemosphere 311, 137012. https://doi.org/10.1016/j.chemosphere.2022.137012.

von Sperling, M., Verbyla, M.E., Oliveira, S.M.A.C., 2020. Assessment of treatment plant performance and water quality data: a guide for students, researchers and practitioners, assessment of treatment plant performance and water quality data: a guide for students, researchers and practitioners. https://doi.org/10.2166/9781780409320.

Wang, J., Zhang, S., Mu, X., Hu, X., Ma, Y., 2022. Research characteristics on cyanotoxins in inland water: insights from bibliometrics. Water (Switzerland) 14, 1–12. https://doi.org/10.3390/w14040667.

Wert, E.C., Korak, J.A., Trenholm, R.A., Rosario-Ortiz, F.L., 2014. Effect of oxidant exposure on the release of intracellular microcystin, MIB, and geosmin from three cyanobacteria species. Water Res. 52, 251–259. https://doi.org/10.1016/j.watres.2013.11.001.

Ye, B., Cang, Y., Li, J., Zhang, X., 2019. Advantages of a ClO₂/NaClO combination process for controlling the disinfection by-products (DBPs) for high algae-laden water. Environ. Geochem. Health 41, 1545–1557. https://doi.org/10.1007/s10653-018-0231-8.

Zamyadi, A., Fan, Y., Daly, R.I., Prévost, M., 2013. Chlorination of *Microcystis aeruginosa*: toxin release and oxidation, cellular chlorine demand and disinfection by-products formation. Water Res. 47, 1080–1090. https://doi.org/10.1016/j.watres.2012.11.031.

Zhang, H., Dan, Y., Adams, C.D., Shi, H., Ma, Y., Eichholz, T., 2017. Effect of oxidant demand on the release and degradation of microcystin-LR from *Microcystis aeruginosa* during oxidation. Chemosphere 181, 562–568. https://doi.org/10.1016/j.chemosphere.2017.04.120.

Zhou, S., Shao, Y., Gao, N., Li, L., Deng, J., Zhu, M., Zhu, S., 2014. Effect of chlorine dioxide on cyanobacterial cell integrity, toxin degradation and disinfection by-product formation. Sci. Total Environ. 482–483, 208–213. https://doi.org/10.1016/j.scitotenv.2014.03.007.